Digital PLL control for single-phase photovoltaic system

J.-W. Choi, Y.-K. Kim and H.-G. Kim

Abstract: Utility-voltage information, such as the frequency, phase angle and amplitude, is very important in many industrial systems. In a three-phase system, the utility-voltage information can easily be obtained using a utility-voltage vector, as the magnitude and angle of the voltage vector indicate the amplitude and angle of the utility voltage, respectively. However, for a single-phase system, the utility-voltage information is much more difficult to acquire. Conventionally, the frequency and phase angle of a single-phase voltage are obtained by detecting the zero-cross point. Yet, this method cannot provide the utility-voltage information instantaneously and is very sensitive to noise. Accordingly, the paper presents a novel digital phase-locked loop (PLL) algorithm for single-phase photovoltaic systems. The algorithm uses two virtual phases, and its performance is demonstrated under various utility conditions to show the effectiveness of the proposed algorithm.

1 Introduction

The frequency and phase angle of the utility voltage represent basic information for an increasing number of grid-connected power-conditioning equipment, such as uninterruptible power supplies (UPS), grid-connected photovoltaic systems, and AC/DC convertors. In such applications, accurate and fast detection of the phase angle of the utility voltage is essential for generating the current-reference signals. Utility-voltage information, including the frequency, phase angle and amplitude is also very important in many industrial systems [1–3]. In a three-phase system, the utility-voltage information can easily be obtained using a utility-voltage vector, as the magnitude and angle of the voltage vector indicate the amplitude and angle of the utility voltage, respectively. However, for a single-phase system, the utility-voltage information is much harder to obtain. Conventionally, the frequency and phase angle of a single-phase voltage are obtained by detecting the zero-cross point. Yet this method is unable to detect the utility-voltage information instantaneously and is very sensitive to noise. Accordingly, this paper presents a novel digital PLL (phase-locked loop) algorithm for single-phase photovoltaic systems. The algorithm uses two virtual phases, and its performance is demonstrated under various utility conditions to show the effectiveness of the proposed algorithm.

2 Zero-cross-detection method

Figure 1 shows the zero-cross-detection method, where the zero-cross point is detected every half period. The estimated angle $\hat{\theta}$ is obtained by integrating the estimated frequency $\hat{\omega}$, which is estimated by controlling the angle difference to zero in the PI controller. In Fig. 1, ω_{set} is the initial frequency value.

Figure 2 shows a flow chart of the zero-cross-detection method, where the currently sampled value for the utility voltage is multiplied by the past sampled period, enabling the zero-crossing point to be detected. If the current value is larger than zero, the phase angle θ is zero; otherwise, the phase angle θ is π. Yet the shortcoming of this method is its sensitivity to noise. If noise is inserted into the utility voltage, a phase-detection error occurs, because the zero-crossing point is passed several times.

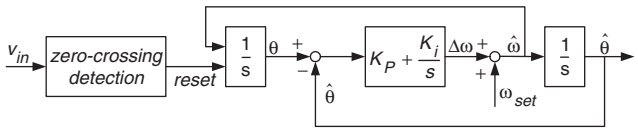

Fig. 1 *Zero-cross-detection method*

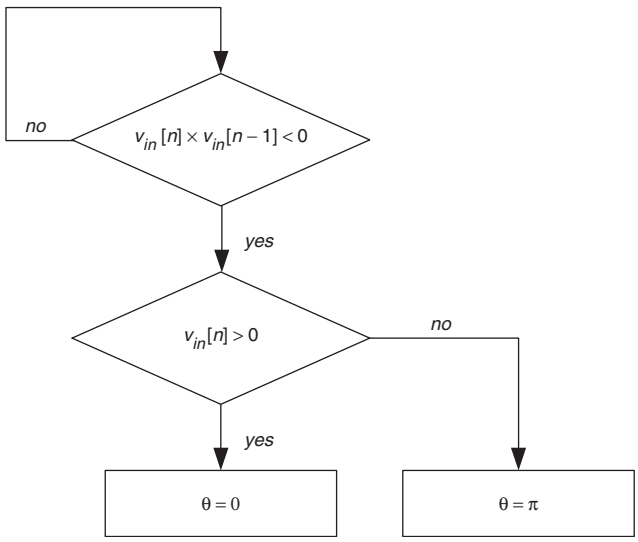

Fig. 2 *Flowchart of zero-cross-detection method*

IEE Proceedings online no. 20045225

doi:10.1049/ip-epa:20045225

Paper first received 12th November 2004 and in final revised form 21st September 2005

The authors are with School of Electronic & Electrical Engineering, Kyungpook National University, Sangyeok-dong, Buk-gu, Daegu, Korea

E-mail: jwchoi@ee.knu.ac.kr

3 Analysis of virtual two-phase detector

Figure 3 shows the virtual two-phase detector, which is divided into two parts. One part is called the two-phase generator, which obtains v_d^s and v_q^s whose phase-angle difference is $\pi/2$. These two signals are then controlled by the second part, called the phase controller. As the result, the estimated phase angle $\hat{\theta}$, estimated frequency $\hat{\omega}$, and estimated amplitude $\hat{E}$ are obtained.

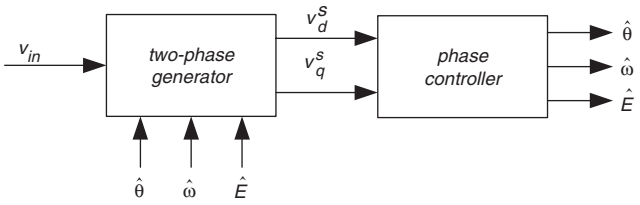

Fig. 3 *Virtual two-phase detector*

3.1 Two-phase generator

In Fig. 3, the input voltage is given by

$$v_{in} = E\sin(\omega t) = E\sin(\theta) \tag{1}$$

The two-phase generator generates v_d^s and v_q^s whose phase-angle difference is $\pi/2$. v_d^s and v_q^s are

$$v_q^s = E\sin(\omega t) = v_{in} \tag{2}$$

$$v_d^s = E\cos(\omega t) \tag{3}$$

(*a*) *Method using memory table [1]*

In Fig. 4, v_{in} is stored in the memory every period. v_q^s is equal to v_{in} and the previous 1/4-period value of v_{in} is multiplied by (-1) and $\omega \cong \hat{\omega}$, then

$$\begin{aligned} v_d^s &= -v_{in}\left(t - \frac{\pi}{2\hat{\omega}}\right) \\ &= -E\sin\left(\omega t - \frac{\omega}{\hat{\omega}}\frac{\pi}{2}\right) \cong E\cos(\omega t) \end{aligned} \tag{4}$$

is given and if $E \cong \hat{E}$ and $\theta \cong \hat{\theta}$, v_d^s and v_q^s whose phase-angle difference is $\pi/2$ are obtained.

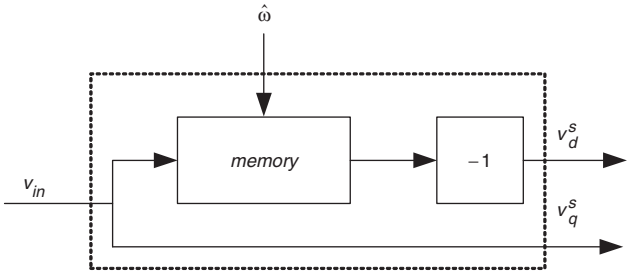

Fig. 4 *Method using memory table*

(*b*) *Method using estimated phase angle and amplitude*

In Fig. 5, the estimated amplitude $\hat{E}$ can be multiplied by $\cos\hat{\theta}$; then

$$v_d^s = \hat{E}\cos\hat{\theta} \cong E\cos\theta \tag{5}$$

(*c*) *Method using second-order filter*

In Fig. 6, v_d^s and v_q^s are obtained using a second-order low-pass filter (LPF). When the input voltage v_{in} passes through the second-order low-pass filter, where the damping ratio $\zeta = 1/\sqrt{2}$, the undamped natural frequency ω_n has the same value as the estimated frequency $\hat{\omega}$, and the estimated

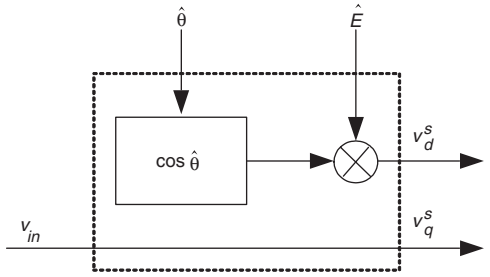

Fig. 5 *Method using estimated phase angle and amplitude*

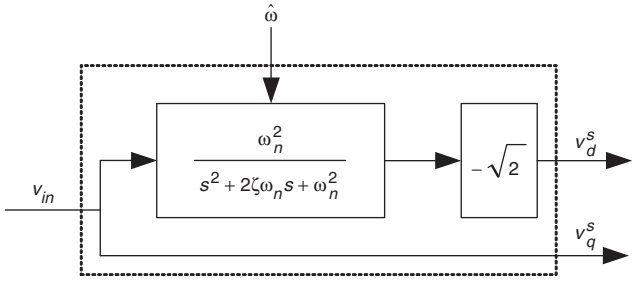

Fig. 6 *Method using second-order low-pass filter*

frequency $\hat{\omega}$ is equal to the real frequency ω, a signal with a phase-angle difference of $\pi/2$ and amplitude of $E/\sqrt{2}$ is obtained. Therefore,

$$v_d^s \cong \left\{(-\sqrt{2})\left(\frac{E}{\sqrt{2}}\sin\left(\omega t - \frac{\pi}{2}\right)\right)\right\} = E\cos(\omega t) \tag{6}$$

is calculated.

(*d*) *Method using first-order filter*

In Fig. 7, v_d^s and v_q^s are obtained using a first-order low-pass filter (LPF). When the input voltage v_{in} passes through the first order low-pass filter, where the cutoff frequency ω_n has the same value as the estimated frequency $\hat{\omega}$ and $\omega \cong \hat{\omega}$, $(E/\sqrt{2})\sin(\omega t - \pi/4)$ is obtained. Therefore, v_d^s is

$$\begin{aligned} v_d^s &= v_{in} - 2\times\frac{E}{\sqrt{2}}\sin\left(\omega t - \frac{\pi}{4}\right) \\ &= E\sin(\omega t) - 2\times\frac{E}{\sqrt{2}}\sin\left(\omega t - \frac{\pi}{4}\right) = E\cos(\omega t) \end{aligned} \tag{7}$$

(*e*) *Method using all-pass filter*

In Fig. 8, v_d^s and v_q^s are obtained using an all-pass filter. When the input voltage v_{in} passes through the all-pass filter, where the damping ratio $\zeta = 1$, the undamped natural frequency ω_n is $(\sqrt{2}-1)$ times as large as the estimated frequency $\hat{\omega}$, and $\omega \cong \hat{\omega}$, a signal with a phase-angle difference of $\pi/2$ and amplitude of E is obtained. Therefore v_d^s is

$$v_d^s = \hat{E}\cos\hat{\theta} \cong E\cos\theta \tag{8}$$

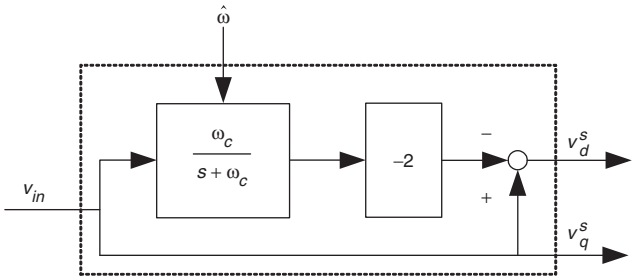

Fig. 7 *Method using first-order low-pass filter*

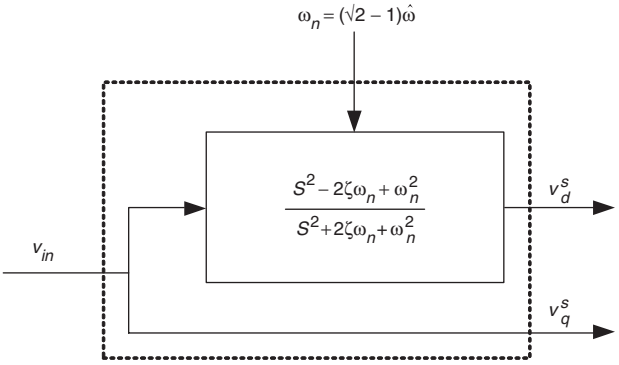

Fig. 8 *Method using all-pass filter*

3.2 Phase controller

In Fig. 3, the phase controller generates the estimated phase angle $\hat{\theta}$, estimated frequency $\hat{\omega}$, and estimated amplitude $\hat{E}$ using v_d^s and v_q^s.

(*a*) *Method using arctangent function*
In Fig. 9,

$$\theta^* = \tan^{-1}\left(\frac{v_q^s}{v_d^s}\right) \tag{9}$$

is obtained. $\Delta\omega$ is obtained by controlling the phase-angle difference $\theta^* - \hat{\theta}$ to zero using the PI loop. $\Delta\omega$ is then added to the initial value ω_{set} to obtain the estimated frequency $\hat{\omega}$. Next, the estimated phase angle $\hat{\theta}$ is obtained by integrating the estimated frequency $\hat{\omega}$. Finally, the estimated amplitude $\hat{E}$ is calculated by

$$\hat{E} = \sqrt{\left\{(v_d^s)^2 + (v_q^s)^2\right\}} \tag{10}$$

When there is a lot of noise, an low-pass filter (LPF) can be inserted to reduce the effect of the noise.

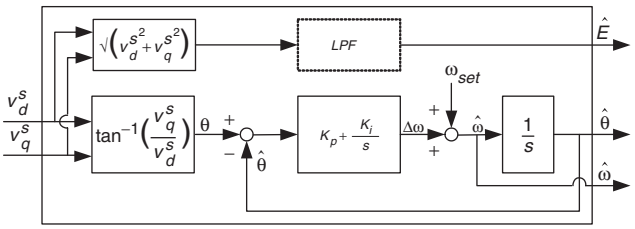

Fig. 9 *Method using arctangent function*

(*b*) *Method using synchronous frame*
In Fig. 10, where v_d^s and v_q^s are converted to a synchronous reference frame,

$$v_d^e = v_d^s \cos\hat{\theta} + v_q^s \sin\hat{\theta} \tag{11}$$

$$v_q^e = -v_d^s \sin\hat{\theta} + v_q^s \cos\hat{\theta} \tag{12}$$

is given. Substituting $v_d^s = E\cos\theta$, $v_q^s = E\sin\theta$ into (10) and (11), when the difference $\hat{\theta} - \theta$ is sufficiently small, the following approximation can be used:

$$v_d^e = E\cos(\hat{\theta} - \theta) \cong E \tag{13}$$

$$v_q^e = E\sin(\theta - \hat{\theta}) \cong E(\theta - \hat{\theta}) \tag{14}$$

In other words, v_d^e expresses the estimated amplitude, while v_q^e expresses the estimated phase-angle error. $\Delta\omega$ is obtained by controlling the estimated phase-angle error using the PI

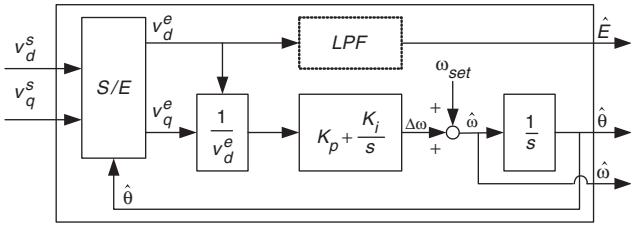

Fig. 10 *Method using synchronous frame*

loop, where v_q^e is divided by the estimated amplitude $\hat{E}$. $\Delta\omega$ is then added to the initial value ω_{set} to obtain the estimated frequency $\hat{\omega}$ and estimated phase angle $\hat{\theta}$. When there is a lot of noise, an LPF can be inserted to reduce the effect of the noise.

3.3 Actual implementation

Figure 11 shows the actual overall configuration. Since an LPF is inserted to reduce the noise, the gain K is multiplied to compensate for any amplitude reduction due to the LPF, while a compensation angle θ_{com} is added to compensate for any phase delay due to the LPF. The transfer function for the LPF is $F(s)$, and the gain K and compensation angle θ_{com} are

$$K = \frac{1}{|F(j\hat{\omega})|} \tag{15}$$

$$\theta_{com} = \angle F(j\hat{\omega}) \tag{16}$$

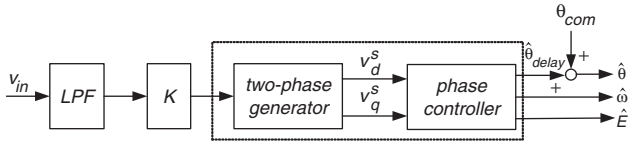

Fig. 11 *Overall configuration*

Table 1: Combination of two-phase generator and phase controller

Method	Two-phase generator	Phase controller
1	method using memory table	method using arctangent function
2	method using the estimated phase angle and amplitude	method using arctangent function
3	method using second-order filter	method using arctangent function
4	method using first-order filter	method using arctangent function
5	method using all-pass filter	method using arctangent function
6	method using memory table	method using synchronous frame
7	method using estimated phase angle and amplitude	method using synchronous frame
8	method using second-order filter	method using synchronous frame
9	method using first-order filter	method using synchronous frame
10	method using all-pass filter	method using synchronous frame

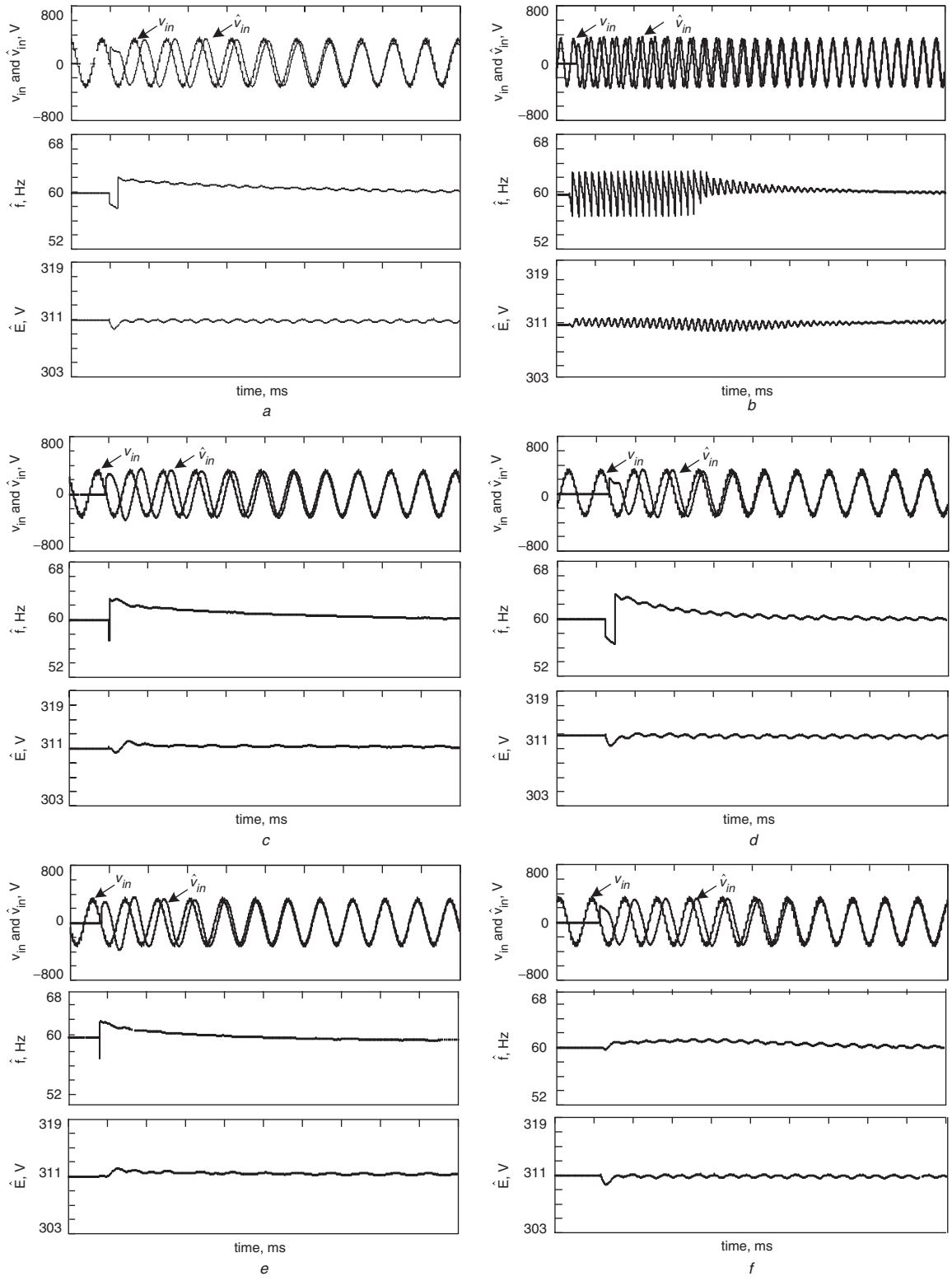

Fig. 12 *Estimation characteristics at start-up*
Top: input voltage v_{in} and estimated input voltage v_{in} (V)
Centre: estimated frequency f (Hz)
Bottom: estimated amplitude E (V)
a Method 1, time 20 ms/division
b Method 2, time 50 ms/division
c Method 3, time 20 ms/division
d Method 4, time 20 ms/division
e Method 5, time 20 ms/division
f Method 6, time 20 ms/division
g Method 7, time 50 ms/division
h Method 8, time 20 ms/division
i Method 9, time 20 ms/division
j Method 10, time 20 ms/division

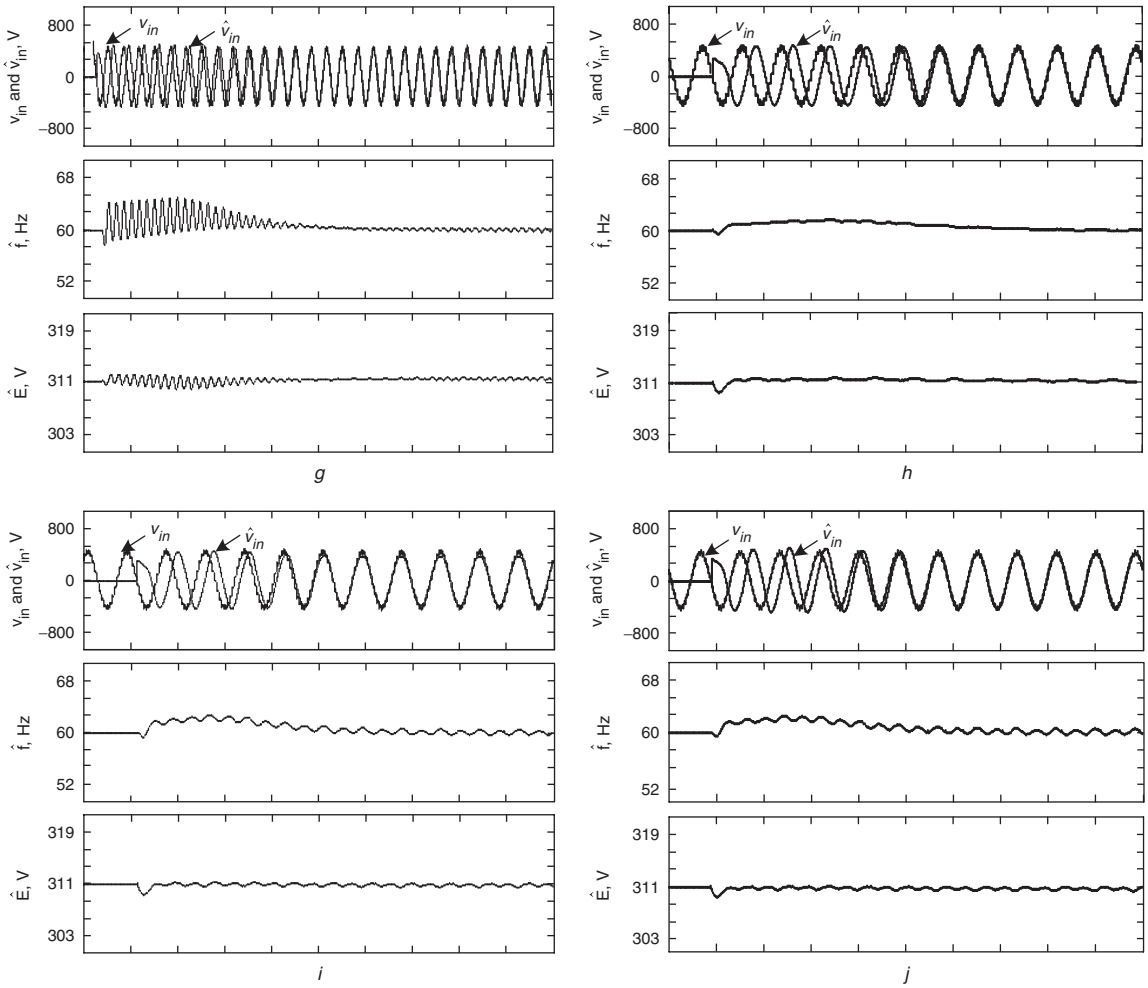

Fig. 12 *Continued*

4 Experiment

When the two-phase generator was combined with the phase controller, ten digital PLL methods were constructed, as shown in Table 1.

Experiments were conducted to evaluate every method as regards its dynamic response, steady-state response, response with a voltage drop and response with the injection of a harmonic component (third and fifth). In the experiments testing the dynamic response, steady-state response, and response with a voltage drop, the amplitude of the input voltage was 220 V RMS, the frequency was 60 Hz, and the amplitude of the injected noise was 30 V peak with a frequency of 1 kHz. The controller started when the real phase angle of the input voltage was π. When injecting a harmonic component, the amplitude of the input voltage was 220 V RMS, the frequency was 60 Hz, and the third- and fifth-harmonic wave components were injected. The following equation was given using the estimated amplitude $\hat{E}$ and estimated phase angle $\hat{\theta}$.

$$\hat{v}_{in} = \hat{E} \sin \hat{\theta} \tag{17}$$

4.1 Dynamic response

Figure 12 shows the dynamic response of the proposed methods. The estimated phase angle, amplitude and frequency were all synchronised to those of the input voltage between 100 ms and 300 ms, as shown in Table 2.

The methods using estimated phase angle and amplitude (2 and 7) are very easy to realise, but they have very poor dynamic-response characteristics. The phase angle was synchronous at 250–300 ms for methods 2 and 7, while the other methods were synchronous at 100–140 ms. The methods that used a memory table (1 and 6) show moderate performance, but they have implementation difficulties requiring large memory size. The methods that used a filter are relatively easy to realise and they have good performance. Methods using first-order low-pass filter (4 and 9) and all-pass filter (5 and 10) show the shortest estimation time and methods using second-order low-pass filter (3 and 8) show less oscillation. The methods using the arctangent function (1–5) are easy to understand but have implementation difficulties in calculating the arctangent function. The methods using a synchronous frame (6–10) are superior to the methods using the arctangent function in implementation. Moreover, in this experiment, they show

Table 2: Comparison of estimation time

Method	1	2	3	4	5	6	7	8	9	10
Estimation time (ms)	120	300	140	100	100	120	250	120	100	100

slightly better performance than the methods using the arctangent function.

In this experiment, the controller starts its work when the real phase angle of the input voltage is π with zero initial condition; i.e., the initial phase-angle error is π. This experiment was therefore performed in the worst case. In the event of a sudden phase-angle increase in the line, the phase-angle error created by the increasing phase angle happens suddenly. This situation is similar to the experiment. So, even with the sudden phase-angle increase, the controller can find the exact angle in a time less than that listed in Table 2.

Actually, the dynamic response of the PLL controllers is heavily dependent on the PI gains in Figs. 9 and 10. Generally, the larger gains improve dynamic response but the system will be more sensitive to noise.

4.2 Steady-state response

Figure 13 shows the steady-state response for the method using the second-order filter for the two-phase generator and the synchronous frame for the phase. In spite of the noise, the amplitude and phase angle for the estimated input voltage were synchronised successfully to those for the real input voltage. Meanwhile, with the other methods, the estimated input voltage successfully tracked the real input voltage, giving similar results.

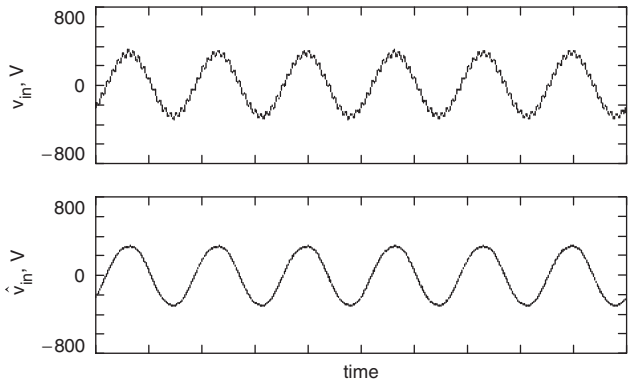

Fig. 13 *Estimated characteristics under steady state*
Top: input voltage v_{in}

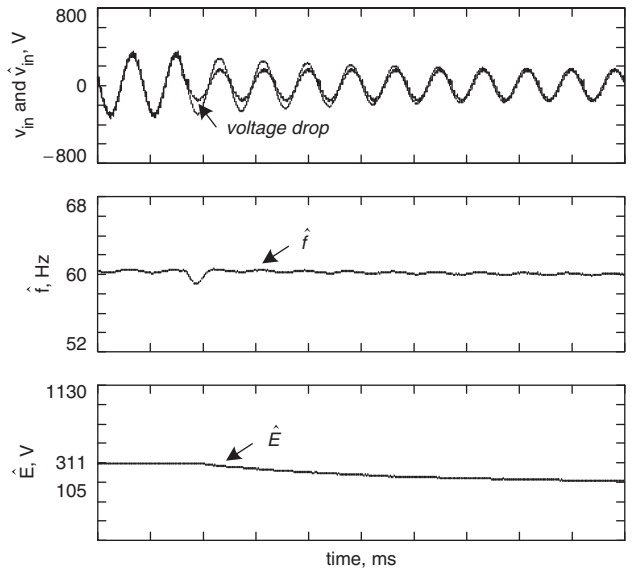

Fig. 14 *Estimation characteristics with voltage drop*
Top: input voltage v_{in} and estimated input voltage v_{in} (V)
Centre: estimated frequency f (Hz)
Bottom: estimated amplitude E (V)
Time: 20 ms/division

4.3 Response with voltage drop

Figure 14 shows the response with a 50% voltage drop when using a second-order filter for the two-phase generator

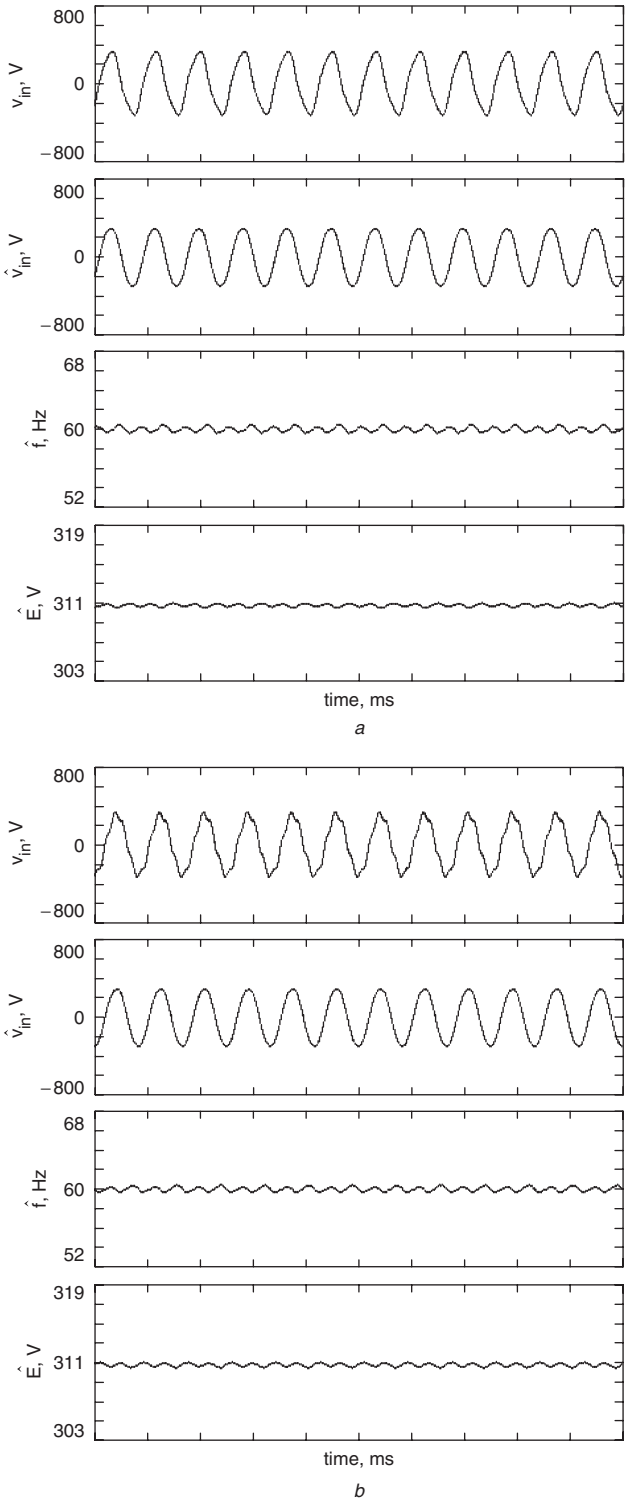

Fig. 15 *Estimation characteristics with injection of third- and fifth-harmonic components*
Top: input voltage v_{in} and estimated input voltage v_{in} (V)
Centre: estimated frequency f (Hz)
Bottom: estimated amplitude E (V)
Time: 20 ms/division
a Injection of third-harmonic component
b Injection of fifth-harmonic component

and synchronous frame for the phase controller. The estimated input was synchronous at 100 ms. With the other methods (apart from methods 2 and 7), the estimated input voltage successfully tracked the real input voltage, giving similar results. The estimated input was synchronous at 250 ms with methods 2 and 7.

According to IEEE standard 929:2000, normal operating conditions for small PV systems are 88–110% of nominal voltage, i.e. 274–342 V in magnitude. For a 50% nominal voltage, the trip time, which is the time between the abnormal condition being applied and the invertor ceasing to energise the utility line, should be less than six cycles. In Fig. 14, the PLL controller detects an abnormal condition (below 274 V) within 20 ms (1.2 cycles), which shows that the dynamic response obtained is sufficient for the required dynamic response in the application.

4.4 Response with injected harmonic component

Figure 15 shows the response with an injected harmonic component (third and fifth) when using a second-order filter for the two-phase generator and a synchronous frame for the phase controller. Meanwhile, with the other methods, the estimated input voltage successfully tracked the real input voltage, giving similar results.

5 Conclusions

A new approach for digital PLL control using a virtual two-phase detector was proposed and verified by experiments. The virtual two-phase detector consists of a two-phase generator and phase controller, and the two phases have five options, while the phase controller has two options. Thus, when the two-phase generator is combined with the phase controller, this provides ten digital-PLL methods. Experimental results demonstrated that the methods using a memory table and filter were superior. However, owing to implementation difficulties with the methods that used a memory table, the methods that used a filter and synchronous frame were found to be preferable.

6 Acknowledgment

This work has been supported by EESRI (R-2002-B-051), which is funded by the Korean Ministry of Commerce Industry and Energy.

7 References

1 Sakamoto, S., Izumi, T., Yokoyama, T., and Haneyoshi, T.: 'A new method for digital PLL control using estimated quadrature two phase frequency detection'. Proc. PCC Osaka, 2002, Vol. 2, pp. 671–676
2 Hsieh, G.-C., and Hung, J.C.: 'Phase-locked loop techniques loop techniques. A survey', *IEEE Trans. Ind. Electron.*, 1996, **43**, (6), pp. 609–615
3 Arruda, L.N., Silva, S.M., and Filho, B.J.C.: 'PLL structures for utility connected systems'. IAS, 2001, Vol. 4, pp. 2655–2660